This is a repository copy of *Density matrix theory of transport and gain in quantum cascade lasers in a magnetic field*.

White Rose Research Online URL for this paper:
http://eprints.whiterose.ac.uk/3433/

Density matrix theory of transport and gain in quantum cascade lasers in a magnetic field

Ivana Savić,* Nenad Vukmirović, Zoran Ikonić, Dragan Indjin, Robert W. Kelsall, and Paul Harrison

School of Electronic and Electrical Engineering, University of Leeds, Leeds LS2 9JT, United Kingdom

Vitomir Milanović

Faculty of Electrical Engineering, University of Belgrade, 11120 Belgrade, Serbia

A density matrix theory of electron transport and optical gain in quantum cascade lasers in an external magnetic field is formulated. Starting from a general quantum kinetic treatment, we describe the intraperiod and interperiod electron dynamics at the non-Markovian, Markovian, and Boltzmann approximation levels. Interactions of electrons with longitudinal optical phonons and classical light fields are included in the present description. The non-Markovian calculation for a prototype structure reveals a significantly different gain spectra in terms of linewidth and additional polaronic features in comparison to the Markovian and Boltzmann ones. Despite strongly controversial interpretations of the origin of the transport processes in the non-Markovian or Markovian and the Boltzmann approaches, they yield comparable values of the current densities.

I. INTRODUCTION

The rapid experimental progress in the field of quantum cascade lasers[1] (QCLs) has initiated considerable theoretical activity to explain the underlying physical phenomena and improve their performance by design optimization. To date, both semiclassical and quantum-mechanical theories of carrier transport in QCLs without magnetic field have been proposed. Semiclassical ones are based on the assumption that coherent processes in QCLs are negligible and electron transport occurs via scattering processes only. They rely on the Boltzmann transport equation, for the solution of which a few approaches may be employed. The Monte Carlo method is a stochastic approach which simulates the trajectories of a representative ensemble of carriers.[2–4] An assumption that the carrier distribution in any particular subband can be approximated by Fermi-Dirac statistics allows the Boltzmann equations to be replaced by simpler and less computationally demanding rate equations.[5,6] Quantum-mechanical models enable the description of phase coherence as well as incoherent scattering processes, and they have been formulated using the density-matrix or nonequilibrium Green's function approach.[7–14] Comparison of the results obtained with the Boltzmann and density matrix approaches in a mid-infrared QCL performed by Iotti *et al.*[7] showed that quantum corrections to the current density are negligible. However, the analysis of gain spectra in the nonequilibrium Green's function description demonstrated that the negligence of coherences between QCL states results in significantly broader linewidths.[12] Also, it has been argued that coherences are not irrelevant for transport in terahertz (THz) QCLs where the small anticrossing energies may allow for resonant tunneling.[15] Moreover, a very recent study[13] gave an interpretation where the current across QCLs is entirely coherent. In addition to the studies concentrated on QCLs, there is mounting theoretical evidence for the presence of quantum coherence features in linear absorption spectra and nonlinear ultrafast optical response for intersubband transitions in unbiased quantum wells (QWs).[16–20]

Furthermore, experimental interest in the QCL performance in a magnetic field has stimulated theoretical efforts to describe the influence of a magnetic field on the physical processes involved. However, since this research topic emerged recently, very few theoretical studies of QCLs in a magnetic field, compared to the amount of those for QCLs without magnetic field, have been reported. Most of them were focused on the modeling of various scattering rates (electron-longitudinal optical phonon,[21–24] electron-electron,[25,26] interface roughness,[27] and alloy disorder[28]) and the calculation of these scattering rates between the upper and the lower laser levels. Modeling of the active region of QCLs, including electron-longitudinal optical (LO) phonon and electron-longitudinal acoustic (LA) phonon scattering, and assuming a unity injection approximation, has also been reported.[29,30] Finally, a semiclassical model of the electron transport in a magnetic field based on the Boltzmann equation has been proposed.[31] Apart from the work done on QCLs in a magnetic field, a few theoretical investigations of QW systems subjected to a magnetic field, based on both the density matrix and nonequilibrium Green's function approaches, have been reported,[32] and confirmed the importance of quantum coherence effects on the ultrafast time scales.[33,34]

Currently, no experimental or theoretical data on coherent phenomena in QCLs in a magnetic field are available. Since the energy spectra in such structures is discrete, it is reasonable to expect that coherent effects are more significant than for QCLs without magnetic field. The aim of this work is to present a quantum-mechanical theory of transport and gain properties of QCLs in an external magnetic field. For that purpose, we derived quantum kinetics equations for QC structures in a magnetic field, based on the density matrix formalism, which include interaction of electrons with LO phonons and optical field. Furthermore, we obtained the corresponding equations in the Markovian approximation, from which the semiclassical Boltzmann transport equations can be recovered. A comprehensive analysis is performed for an example GaAs/Al$_{0.3}$Ga$_{0.7}$As QCL and nonequilibrium steady state results obtained from all three approaches (quantum kinetic, Markovian, and Boltzmann) are compared.

II. THEORETICAL CONSIDERATIONS

A. Quantum kinetic equations

We consider electrons in the conduction band of a QCL in a magnetic field applied in the direction perpendicular to QW layers (z axis). Such a magnetic field splits the in-plane continuum of quantized subbands into Landau levels (LLs), additionally described by Landau and spin indices.[35] Within the effective mass and envelope function approximations, and neglecting the spin splitting, the energy of the j_ith LL originated from the m_ith state (subband), in further considerations denoted with a shorthand subscript i, $i = |m_i, j_i\rangle$, reads

$$E_i = E_{|m_i,j_i\rangle} = \bar{E}_{m_i} + \left(j_i + \frac{1}{2}\right)\frac{\hbar eB}{m^*}, \quad (1)$$

where $\bar{E}_{m_i}$ is the energy of state m_i, $\hbar$ is the reduced Planck's constant, e is the electron charge, B is the applied magnetic field, and m^* is the electron effective mass (taken to be equal to 0.067 in free electron mass units). For the magnetic vector potential $\mathbf{A}$ given in the Landau gauge ($\mathbf{A} = Bx\mathbf{e}_y$), the envelope wave function of the ith LL takes the form

$$\Psi_{i,k}(\mathbf{r}) = u_{j_i}[x - f(k)]\psi_{m_i}(z)\frac{e^{iky}}{\sqrt{L_y}}, \quad (2)$$

where k is the wave vector of the electron, $u_{j_i}[x - f(k)]$ is the wave function of the harmonic oscillator with $f(k) = k/(eB/\hbar)$, $\psi_{m_i}(z)$ is the wave function of the m_ith size-quantized state, and L_y is the dimension of the structure along the y axis.

The model Hamiltonian of the system described above reads as follows:

$$\hat{H} = \hat{H}_0 + \hat{H}_{el} + \hat{H}_{ep}. \quad (3)$$

The first term represents the Hamiltonian of noninteracting electrons and phonons in applied electric and magnetic fields. The second and the third term describe electron-light and electron-LO phonon interactions, respectively. In this first step towards formulating a density matrix theory of QCLs in a magnetic field, we do not consider other interaction mechanisms of electrons (with LA phonons, ionized impurities, interface defects, and other electrons). The Hamiltonian of free electrons and phonons reads as follows:

$$\hat{H}_0 = \sum_{i,k} E_i \hat{c}_{i,k}^\dagger \hat{c}_{i,k} + \sum_{\mathbf{q}} E_{\mathbf{q}} \hat{b}_{\mathbf{q}}^\dagger \hat{b}_{\mathbf{q}}, \quad (4)$$

where E_i is the energy of the ith electron state, $E_{\mathbf{q}}$ is the energy of the phonon of a wave vector $\mathbf{q}$, and $\hat{c}_{i,k}^\dagger$ ($\hat{b}_{\mathbf{q}}^\dagger$) and $\hat{c}_{i,k}$ ($\hat{b}_{\mathbf{q}}$) represent creation and annihilation operators of the electron (phonon), respectively. The electron-light interaction in the dipole approximation is given by the following Hamiltonian:

$$\hat{H}_{el} = \sum_{i,j,k,k'} e\mathbf{A}_R \mathbf{V}_{ij}^{kk'} \hat{c}_{i,k}^\dagger \hat{c}_{j,k'}, \quad (5)$$

where $\mathbf{A}_R$ represents the magnetic vector potential of a monochromatic light wave incident on a QW structure, given

in the Coulomb gauge, and the velocity matrix element is found according to

$$\mathbf{V}_{ij}^{kk'} = \int d\mathbf{r}\Psi_{i,k}^*(\mathbf{r})\hat{\mathbf{v}}_0\Psi_{j,k'}(\mathbf{r}). \quad (6)$$

The velocity operator for the nonilluminated system $\hat{\mathbf{v}}_0$ may be represented as

$$\hat{\mathbf{v}}_0 = \frac{1}{m^*}\hat{\mathbf{p}} + \frac{e\mathbf{A}}{m^*}, \quad (7)$$

where $\hat{\mathbf{p}}$ is the momentum operator. The Hamiltonian describing the electron-phonon interaction can be cast in the form[36,37]

$$\hat{H}_{ep} = \sum_{i,j,k,k',\mathbf{q}} (g_{k,\mathbf{q},k'}^{ij}\hat{c}_{i,k}^\dagger\hat{b}_{\mathbf{q}}\hat{c}_{j,k'} + g_{k,\mathbf{q},k'}^{ij*}\hat{c}_{j,k'}^\dagger\hat{b}_{\mathbf{q}}^\dagger\hat{c}_{i,k}), \quad (8)$$

with

$$g_{k,\mathbf{q},k'}^{ij} = g_{\mathbf{q}}\int d\mathbf{r}\Psi_{i,k}^*(\mathbf{r})e^{i\mathbf{q}\cdot\mathbf{r}}\Psi_{j,k'}(\mathbf{r}), \quad (9)$$

where $g_{\mathbf{q}}$ represents the coupling factor. For the electron-LO phonon interaction, the coupling factor reads

$$g_{\mathbf{q}} = -ie\left(\frac{\hbar\omega_{LO}}{2V}(\epsilon_\infty^{-1} - \epsilon_s^{-1})\right)^{1/2}\frac{1}{q}, \quad (10)$$

where the energy of each phonon mode is considered to be approximately constant ($\hbar\omega_{LO}$), V is the volume, and ϵ_∞ and ϵ_s are high-frequency and static permittivity, respectively. In the case of QWs in a magnetic field, the phonon coupling factor $g_{k,\mathbf{q},k'}^{ij}$ may be written as

$$g_{k,\mathbf{q},k'}^{ij} = g_{\mathbf{q}}\int d\mathbf{r}u_{j_i}^*[x - f(k)]\frac{e^{-iky}}{\sqrt{L_y}}\psi_{m_i}^*(z)e^{i(q_x x + q_y y + q_z z)}$$

$$\times u_{j_j}[x - f(k')]\frac{e^{ik'y}}{\sqrt{L_y}}\psi_{m_j}(z)$$

$$= g_{\mathbf{q}}\int dy\frac{e^{-i(k-q_y-k')y}}{L_y}\int dx u_{j_i}^*[x - f(k)]e^{iq_x x}$$

$$\times u_{j_j}[x - f(k')]\int dz\psi_{m_i}^*(z)e^{iq_z z}\psi_{m_j}(z)$$

$$= g_{\mathbf{q}}\delta_{k',k-q_y}H_{j_ij_j}(k,k',q_x)G_{m_im_j}(q_z), \quad (11)$$

where $H_{j_ij_j}(k,k',q_x) = \int dx u_{j_i}^*[x - f(k)]e^{iq_x x}u_{j_j}[x - f(k')]$ is the lateral overlap integral and $G_{m_im_j}(q_z) = \int dz\psi_{m_i}^*(z)e^{iq_z z}\psi_{m_j}(z)$ is the form factor.

In the density matrix approach, single particle density matrices like the intraband electron density matrices $f_{i_1i_2,k} = \langle\hat{c}_{i_1,k}^\dagger\hat{c}_{i_2,k}\rangle$ or the phonon occupation number $n_{\mathbf{q}} = \langle\hat{b}_{\mathbf{q}}^\dagger\hat{b}_{\mathbf{q}}\rangle$ represent fundamental physical quantities. Their diagonal elements determine the occupation probabilities of the states, while the nondiagonal elements correspond to the electron polarizations between two states, and are related to the property of quantum-mechanical coherence (superposition). In this work, a thermal equilibrium of phonons is assumed,

hence equations of motion for electron density matrices are sufficient for the description of the system.

In the derivation of the time evolution of single particle density matrices, one starts with the Heisenberg equation of motion.[36,37] The time evolution due to the Hamiltonian of noninteracting electrons and phonons is given as[36,37]

$$\frac{d}{dt} f_{i_1 i_2, k} \bigg|_{\hat{H}_0} = \frac{1}{i\hbar}(E_{i_2} - E_{i_1}) f_{i_1 i_2, k}. \qquad (12)$$

The equation of motion in the case of interaction of electrons with light polarized in the z direction reads[36–38]

$$\frac{d}{dt} f_{i_1 i_2, k} \bigg|_{\hat{H}_{el}} = \frac{e}{i\hbar} \sum_{i_3} A_R (V_{i_2 i_3} f_{i_1 i_3, k} - V_{i_3 i_1} f_{i_3 i_2, k}), \qquad (13)$$

with the z component of the velocity matrix element

$$V_{i_1 i_2} = \frac{i}{\hbar}(E_{i_1} - E_{i_2}) z_{i_1 i_2} \delta_{j_{i_1}, j_{i_2}}, \qquad (14)$$

where $z_{i_1 i_2}$ is the matrix element of the operator of the z coordinate. In the present analysis we do not consider any optical-cavity effect and look for nonequilibrium steady state populations and polarizations when $A_R = 0$. However, the electron-light interaction is essential for the calculation of optical gain.

In the quantum kinetics equations for the electron-phonon interaction, phonon-assisted matrices, given by expectation values of three operators $s_{k,\mathbf{q},k'}^{i_1 i_2} = \langle \hat{c}_{i_1,k}^\dagger \hat{b}_{\mathbf{q}} \hat{c}_{i_2,k'} \rangle$, appear, which correlate an initial state consisting of one electron in the state i_2, k' and a phonon with a wave vector $\mathbf{q}$ to a final state with only one electron in the state i_1, k.[36,37] Furthermore, the temporal evolution for the phonon-assisted matrices involves expectation values of four operators, and so on. The resulting infinite hierarchy of equations needs to be truncated in order to access the problem numerically. The first-order contribution, obtained by neglecting all correlations between electrons and phonons in the spirit of the correlation expansion approach[36,37] $(s_{k,\mathbf{q},k'}^{i_1 i_2} \approx \langle \hat{c}_{i_1,k}^\dagger \hat{c}_{i_2,k} \rangle \langle \hat{b}_{\mathbf{q}_{xz}} \rangle \delta_{k',k} \delta_{q_y,0} = f_{i_1 i_2,k} B_{\mathbf{q}_{xz}} \delta_{k',k} \delta_{q_y,0})$, vanishes if a thermal equilibrium of phonons is assumed.[16] The next order in the hierarchy is obtained by taking into account deviations of the phonon-assisted density matrices from the first-order factorization $\delta s_{k,\mathbf{q},k'}^{i_1 i_2} = s_{k,\mathbf{q},k'}^{i_1 i_2} - f_{i_1 i_2,k} B_{\mathbf{q}_{xz}} \delta_{k',k} \delta_{q_y,0}$. Then, the following equations for $\delta s_{k,\mathbf{q},k'}^{i_1 i_2}$ are obtained:[36,37]

$$\frac{d}{dt} \delta s_{k,\mathbf{q},k'}^{i_1 i_2} = \frac{1}{i\hbar}(E_{i_2} + \hbar\omega_{LO} - E_{i_1}) \delta s_{k,\mathbf{q},k'}^{i_1 i_2} - \gamma \delta s_{k,\mathbf{q},k'}^{i_1 i_2}$$

$$+ \frac{1}{i\hbar} \sum_{i_4,i_5} g_{k,\mathbf{q},k'}^{i_5 i_4 *} [(n_0 + 1) f_{i_1 i_5,k} (\delta_{i_4,i_2} - f_{i_4 i_2,k'})$$

$$- n_0 f_{i_4 i_2,k'}(\delta_{i_1,i_5} - f_{i_1 i_5,k})],$$

$$\frac{d}{dt} f_{i_1 i_2, k} \bigg|_{\hat{H}_{ep}} = \frac{1}{i\hbar} \sum_{i_3,k',\mathbf{q}} (g_{k,\mathbf{q},k'}^{i_2 i_3} \delta s_{k,\mathbf{q},k'}^{i_1 i_3} + g_{k',\mathbf{q},k}^{i_3 i_2 *} \delta s_{k',\mathbf{q},k}^{i_3 i_1 *}$$

$$- g_{k',\mathbf{q},k}^{i_3 i_1} \delta s_{k',\mathbf{q},k}^{i_3 i_2} - g_{k,\mathbf{q},k'}^{i_1 i_3 *} \delta s_{k,\mathbf{q},k'}^{i_2 i_3 *}), \qquad (15)$$

where n_0 denotes the equilibrium phonon density given by the Bose-Einstein factor. The terms in the equation for $\delta s_{k,\mathbf{q},k'}^{i_1 i_2}$ are due to the Hamiltonian of free electrons, and of electron-LO phonon interaction, respectively. The equations for phonon-assisted matrices should, in principle, contain a term which describes their time evolution due to the electron-light interaction, here relevant only for the calculation of linear optical gain. However, the coupling of the light field to the phonon-assisted matrices in QWs is a higher-order effect[32] and may be neglected.[18,19] Its inclusion for complex structures like QCLs in a magnetic field would result in a computationally inaccessible task.[33]

Insertion of higher-order terms in the equations for phonon-assisted density matrices should be performed in a self-consistent manner;[39] however, in the system considered, with several subbands and LLs originating from them in each period of the cascade, this would be extremely computationally involved.[36,37] Conversely, discarding these effects leads to numerical instabilities in the actual computation. Therefore, a phenomenological damping constant γ was introduced, representing higher-order correlations,[18,19] which describe collisional broadening of LLs.[37] We have verified that the convergence of our results may be achieved for sufficiently large values of γ ($\hbar\gamma \sim 1$ meV).

It is shown in Appendix A that, in the present description, $f_{i_1 i_2,k}$ is constant for all values of the wave vector k, and may be expressed as $f_{i_1 i_2,k} = \alpha_B n_{i_1 i_2}$, where $\alpha_B = \pi\hbar/eB$ and $n_{i_1 i_2} = \sum_{k'} f_{i_1 i_2,k'}/L_x L_y$. The diagonal element n_{ii} represents the electron sheet density in the ith LL. From the derivation given in Appendix A, the quantum kinetics equations including all the aforementioned interactions amount to

$$\frac{d}{dt} n_{i_1 i_2} = \frac{1}{i\hbar}(E_{i_2} - E_{i_1}) n_{i_1 i_2} + \frac{e}{i\hbar} \sum_{i_3} A_R(V_{i_2 i_3} n_{i_1 i_3} - V_{i_3 i_1} n_{i_3 i_2}) + \frac{1}{i\hbar} \sum_{i_3,i_4,i_5} (W_{i_2 i_3 i_4 i_5} \delta K_{i_1 i_3 i_4 i_5} + W_{i_3 i_2 i_5 i_4}^* \delta K_{i_3 i_1 i_5 i_4}^* - W_{i_3 i_1 i_5 i_4} \delta K_{i_3 i_2 i_5 i_4}$$

$$- W_{i_1 i_3 i_4 i_5}^* \delta K_{i_2 i_3 i_4 i_5}^*),$$

$$\frac{d}{dt} \delta K_{i_1 i_2 i_4 i_5} = \frac{1}{i\hbar}(E_{i_2} + \hbar\omega_{LO} - E_{i_1}) \delta K_{i_1 i_2 i_4 i_5} - \gamma \delta K_{i_1 i_2 i_4 i_5} + \frac{1}{i\hbar}[(n_0 + 1) n_{i_1 i_5}(\delta_{i_4,i_2} - \alpha_B n_{i_4 i_2}) - n_0 n_{i_4 i_2}(\delta_{i_1,i_5} - \alpha_B n_{i_1 i_5})], \qquad (16)$$

$$W_{i_1 i_3 i_4 i_5} = \frac{e^2 \hbar \omega_{LO}}{8\pi^2}(\epsilon_\infty^{-1} - \epsilon_s^{-1}) \sum_{i_3 i_4} \int_{q_{xy}=0}^\infty \int_{q_z=-\infty}^\infty q_{xy} dq_{xy} dq_z \frac{1}{q_{xy}^2 + q_z^2} |H_{j_{i_1} j_{i_3}}(q_{xy})| |H_{j_{i_5} j_{i_4}}(q_{xy})| G_{m_{i_1} m_{i_3}}(q_z) G_{m_{i_5} m_{i_4}}^*(q_z) \delta_{j_{i_1} + j_{i_4}, j_{i_3} + j_{i_5}},$$

with the quantities $\delta K_{i_1 i_2 i_4 i_5}$ associated with the phonon-assisted matrices $\delta s_{k,\mathbf{q},k-q_y}^{i_1 i_2}$ through

$$\delta s_{k,\mathbf{q},k-q_y}^{i_1 i_2} = \sum_{i_4,i_5} g_{\mathbf{q}}^* H_{j_{i_5} j_{i_4}}^*(k, k-q_y, q_x) G_{m_{i_5} m_{i_4}}^*(q_z) \delta K_{i_1 i_2 i_4 i_5}. \tag{17}$$

The quantum-kinetic dynamics is essentially non-Markovian, since the time evolution of the density matrix elements depends on their values at earlier times, i.e., on the memory of the system.

From discussion in Appendix A it follows that the time evolution of electron populations and polarizations in the Markovian approximation may take the form

$$\begin{aligned}
\frac{d}{dt} n_{i_1 i_2} &= \frac{1}{i\hbar}(E_{i_2} - E_{i_1}) n_{i_1 i_2} + \frac{e}{i\hbar}\sum_{i_3} A_R(V_{i_2 i_3} n_{i_1 i_3} - V_{i_3 i_1} n_{i_3 i_2}) \\
&\quad + \sum_{i_3 i_4 i_5} [-\Gamma_{i_2 i_3 i_4 i_5}^{\text{out}} n_{i_1 i_5}(\delta_{i_4,i_3} - \alpha_B n_{i_4 i_3}) \\
&\quad - \Gamma_{i_1 i_3 i_4 i_5}^{\text{out}*} n_{i_2 i_5}^*(\delta_{i_4,i_3} - \alpha_B n_{i_4 i_3}^*) \\
&\quad + \Gamma_{i_2 i_3 i_4 i_5}^{\text{in}} n_{i_4 i_3}(\delta_{i_1,i_5} - \alpha_B n_{i_1 i_5}) \\
&\quad + \Gamma_{i_1 i_3 i_4 i_5}^{\text{in}*} n_{i_4 i_3}^*(\delta_{i_2,i_5} - \alpha_B n_{i_2 i_5}^*)],
\end{aligned}$$

$$\begin{aligned}
\Gamma_{i_1 i_3 i_4 i_5}^{\text{out}} &= \frac{\pi}{\hbar}[\delta(-E_{i_5} + \hbar\omega_{\text{LO}} + E_{i_4}) W_{i_1 i_3 i_4 i_5}(n_0 + 1) \\
&\quad + \delta(-E_{i_5} - \hbar\omega_{\text{LO}} + E_{i_4}) W_{i_3 i_1 i_5 i_4}^* n_0],
\end{aligned}$$

$$\begin{aligned}
\Gamma_{i_1 i_3 i_4 i_5}^{\text{in}} &= \frac{\pi}{\hbar}[\delta(-E_{i_5} + \hbar\omega_{\text{LO}} + E_{i_4}) W_{i_1 i_3 i_4 i_5} n_0 \\
&\quad + \delta(-E_{i_5} - \hbar\omega_{\text{LO}} + E_{i_4}) W_{i_3 i_1 i_5 i_4}^*(n_0 + 1)]. \tag{18}
\end{aligned}$$

Terms $\Gamma_{i_1 i_3 i_4 i_5}^{\text{out/in}}$ have a similar form as scattering rates in the Boltzmann approach, and hence may be referred to as generalized out or in scattering rates. The Markovian approximation neglects the memory time of a scattering process, which is related to energy-time uncertainty.[36,37,39] Scattering and dephasing processes are then restricted only to energy conserving transitions between single-particle states. For discrete energy spectra in QWs in a magnetic field, the electron-LO phonon interaction is thus almost fully suppressed, if broadening is not taken into account. A Lorentzian with the full width at half-maximum (FWHM) of $2\hbar\gamma$ should be used to model the LL broadening in the Markovian description, where γ is the damping parameter introduced in the quantum kinetic description (see Ref. 36 and Appendix A). In the semiclassical limit, which may be obtained by neglecting nondiagonal matrix elements,[36,37] the Markovian equations derived reduce to the Boltzmann equations given in Ref. 31.

Due to the periodicity of the QCL structure, its energy states are invariant upon translation per potential drop across a period, while the wave functions are invariant upon translation per period length. Therefore, each period has an identical set of N LLs, with identical density matrix elements $(n_{i_1 i_2} = n_{(i_1+kN)(i_2+kN)}, \ k=0,\pm 1,\pm 2,\ldots)$, and phonon-assisted matrices $(\delta K_{i_1 i_2 i_3 i_4} = \delta K_{(i_1+kN)(i_2+kN)(i_3+kN)(i_4+kN)})$. This also accounts for the quantities characterizing the scattering processes $(\Gamma_{i_1 i_2 i_3 i_4} = \Gamma_{(i_1+kN)(i_2+kN)(i_3+kN)(i_4+kN)}, W_{i_1 i_2 i_3 i_4} = W_{(i_1+kN)(i_2+kN)(i_3+kN)(i_4+kN)})$ and the velocity operator $(V_{i_1 i_2} = V_{(i_1+kN)(i_2+kN)})$. Since the wave functions are well localized within their periods, the tight-binding description may be introduced, by accounting for the interaction between the nearest-neighboring periods only. Hence, we consider the density matrix elements which couple LLs within one period, as well as the elements which couple those LLs with LLs belonging to the nearest-neighboring periods. Also, we take into account those quantities $W_{i_{1,2} i_3 i_4 i_5}$ and $\Gamma_{i_{1,2} i_3 i_4 i_5}$ with the property that $i_{1,2}$ and i_3 belong to the same or adjacent periods, as well as i_4 and i_5, see Eq. (16), and write Eqs. (16) and (18) for all possible combinations of indices $i_1 - i_5$ which satisfy these conditions. After exploiting the property of shift invariance of all the aforementioned quantities, the system of equations in the quantum-kinetic and/or Markovian approach may be reduced to contain only the density matrix elements of interest. Again, the Boltzmann expressions may be recovered from the Markovian ones.

In the quantum-kinetic and Markovian representations, the number of density matrix elements to be calculated is of the order of N^2, and the number of quantities associated with the phonon-assisted matrices (the quantum kinetics case only) and scattering rates is of the order of N^4. Obviously, the calculation of population and polarization dynamics for the QCLs with many energy states and LLs stemming from them is extremely challenging. Therefore, in our analysis, we restrict ourselves to the case of a QCL with a small number of energy levels per period and subjected to relatively large magnetic fields, characterized by a small number of LLs stemming from those levels which are relevant for transport. Here we took the 10 lowest LL indices, after checking that this number of LLs is sufficient for the considered structure.

A stationary solution of Eqs. (16) and (18) is found by tracking their time evolution, starting from an initial condition that all electrons are in the fundamental ground-state LL (and hence all the polarizations and phonon-assisted matrices are equal to zero), and integrating in time until the steady state is reached. This method proved to be extremely reliable in terms of convergence for solving large systems of nonlinear equations, in contrast to gradient-based methods. The integration is performed by using a Runge-Kutta method with adaptive step size control, which considerably speeds up the process.

Since the quantities associated with the scattering processes $W_{i_1 i_2 i_3 i_4}$ and $\Gamma_{i_1 i_2 i_3 i_4}$ are different from zero only if the condition $j_{i_1} + j_{i_3} = j_{i_2} + j_{i_4}$ is fulfilled, our choice of an initial condition leads to the steady-state solution in which the polarizations $n_{i_1 i_2}$ are not equal to zero only if $j_{i_1} = j_{i_2}$. Although this result may, at first, seem to be a peculiarity of the initial condition, it can also be regarded as a solution of the reduced description of the systems of Eqs. (16) or (18), which includes only those density matrix elements $n_{i_1 i_2}$ with $j_{i_1} = j_{i_2}$.

Careful examination of Eqs. (16) and (18) suggests that, if the terms such as $\alpha_B n_{i_4 i_3}$, $j_{i_4} \neq j_{i_3}$, are much smaller than 1 (i.e., $\delta_{i_4 i_3}$ for $i_4 = i_3$), the terms such as $n_{i_1 i_5}$, $j_{i_1} \neq j_{i_5}$ do not influence the time evolution of the elements $n_{i_1 i_2}$, $j_{i_1} = j_{i_2}$. Therefore, in the lowest order approximation, the analysis of the density matrix dynamics may be limited to the terms $n_{i_1 i_2}$, $j_{i_1} = j_{i_2}$.

B. Current density

The current density may be estimated from the expectation value of the carrier drift velocity $\hat{v}$ (Ref. 11),

$$J = \langle \hat{J} \rangle = -\frac{e}{V} \langle \hat{v} \rangle. \tag{19}$$

In the density matrix formalism, the drift velocity may be calculated according to[9]

$$\langle \hat{v} \rangle = \sum_{i_1, i_2, k} v_{i_1 i_2} f_{i_2 i_1, k}, \tag{20}$$

where $v_{i_1 i_2}$ is the drift velocity matrix element given by

$$v_{i_1 i_2} = \langle i_1 | \hat{v} | i_2 \rangle = \frac{i}{\hbar} \langle i_1 | [\hat{H}, \hat{z}] | i_2 \rangle. \tag{21}$$

The drift velocity density matrix elements then read

$$v_{i_1 i_2} = \frac{i}{\hbar} (E_{i_1} - E_{i_2}) z_{i_1 i_2} + \frac{1}{m^*} e A_R \delta_{i_1, i_2}. \tag{22}$$

The first term is due to the Hamiltonian of noninteracting electrons, while the second one is due to the electron-light interaction. Since the scattering potential of any interaction (electron-phonon, electron-electron, etc.) depends only on the position $\hat{r}$ and not on the momentum $\hat{p}$, it follows that $[\hat{H}_{ep}, \hat{z}] = 0$, and its contribution to the drift velocity vanishes. Starting from Eqs. (19) and (20), and using the assumption that only the density matrix elements between LLs within a period or LLs localized in that period and its nearest neighbors are not zero, the current density finally may be written in the form

$$J = -\frac{e}{d} \sum_{i_1, i_2 = 1}^{N} (v_{i_1 i_2} n_{i_2 i_1} + v_{i_1 (i_2+N)} n_{(i_2+N) i_1} + v_{(i_2+N) i_1} n_{i_1 (i_2+N)}), \tag{23}$$

where d is the length of a period. The Boltzmann expression for the current density may be derived from Eq. (23) by representing the nondiagonal density matrix elements, in the first-order approximation, in terms of the diagonal ones[40]

$$J = \frac{e}{d} \left(\sum_{\substack{i,f=1 \\ (i<f)}}^{N} (z_f - z_i)[n_i W_{if}(1 - \alpha_B n_f) - n_f W_{fi}(1 - \alpha_B n_i)] \right.$$
$$+ \sum_{i,f=1}^{N} (z_{f+N} - z_i)[n_i W_{i(f+N)}(1 - \alpha_B n_f)$$
$$\left. - n_f W_{(f+N)i}(1 - \alpha_B n_i)] \right), \tag{24}$$

where $n_i = n_{ii}$ represents the population of the ith LL and $z_i = z_{ii} = \langle i | z | i \rangle$.

C. Gain spectra

The gain spectra in the quantum-kinetic (non-Markovian) description and in the Markovian approximation may be estimated from the linear response of nonequilibrium stationary populations and polarizations to a small optical perturbation. The relationship between the linear variations in the polarization due to the applied optical field $\Delta P(\omega)$ and the current density $\Delta J(\omega)$ gives the following expression for the susceptibility:[11]

$$\chi(\omega) = \frac{\Delta P(\omega)}{\epsilon_0 E(\omega)} = -\frac{i}{\epsilon_0} \frac{\Delta J(\omega)}{\omega E(\omega)}. \tag{25}$$

The gain coefficient then may be found from[39]

$$g(\omega) = -\frac{\omega}{c} \frac{\text{Im}[\chi(\omega)]}{n}, \tag{26}$$

where n is the refractive index of the system material.

If the Fourier transform of the electric field of light is given by

$$\mathbf{E}(t) = \mathbf{e}_z \int \frac{d\omega}{2\pi} E(\omega) e^{-i\omega t}, \tag{27}$$

then the Fourier transform of the corresponding magnetic vector potential in the Coulomb gauge is represented as

$$\mathbf{A}_R(t) = \mathbf{e}_z \int \frac{d\omega}{2\pi} \frac{E(\omega)}{i\omega} e^{-i\omega t}. \tag{28}$$

The linear changes of intraperiod elements in the frequency domain $\Delta n_{i_1 i_2}(\omega)$, for the quantum kinetics case, may be written as

$$-i\omega \Delta n_{i_1 i_2}(\omega) = \frac{E_{i_2} - E_{i_1}}{i\hbar} \Delta n_{i_1 i_2}(\omega) + \frac{e}{i\hbar} A_R(\omega) \sum_{i_3} \left(V_{i_2 i_3} n_{i_1 i_3}^0 \right.$$
$$- V_{i_3 i_1} n_{i_3 i_2}^0) + \frac{1}{i\hbar} \sum_{i_3, i_4, i_5} [W_{i_2 i_3 i_4 i_5} \Delta K_{i_1 i_3 i_4 i_5}(\omega)$$
$$+ W_{i_3 i_2 i_5 i_4}^* \Delta K_{i_3 i_1 i_5 i_4}^*(-\omega)$$
$$- W_{i_3 i_1 i_5 i_4} \Delta K_{i_3 i_2 i_5 i_4}(\omega)$$
$$\left. - W_{i_1 i_3 i_4 i_5}^* \Delta K_{i_2 i_3 i_4 i_5}^*(-\omega) \right], $$

$$\Delta K_{i_1 i_2 i_3 i_4}(\omega) = -\frac{1}{E_{i_2} + \hbar \omega_{\text{LO}} - E_{i_1} - \hbar \omega - i\hbar \gamma}((n_0 + 1)$$
$$\times \{\Delta n_{i_1 i_4}(\omega) \delta_{i_3, i_2} - \alpha_B [n_{i_1 i_4}^0 \Delta n_{i_3 i_2}(\omega)$$
$$+ n_{i_3 i_2}^0 \Delta n_{i_1 i_4}(\omega)]\} - n_0 \{\Delta n_{i_3 i_2}(\omega) \delta_{i_1, i_4}$$
$$- \alpha_B [n_{i_1 i_4}^0 \Delta n_{i_3 i_2}(\omega) + n_{i_3 i_2}^0 \Delta n_{i_1 i_4}(\omega)]\}), \tag{29}$$

where $n^0_{i_1 i_2}$ represents the steady-state value of the density matrix element between LLs i_1 and i_2. Similar equations which include all possible combinations of $i_1–i_5$ as discussed in Section II A also need to be taken into account. In the Markovian case, taking into consideration the property of the density matrix elements that $n_{i_2 i_1}(t) = n^*_{i_1 i_2}(t)$, the equations of motion of intraperiod density matrix elements transform to the frequency domain according to

$$-i\omega \Delta n_{i_1 i_2}(\omega) = \frac{E_{i_2} - E_{i_1}}{i\hbar} \Delta n_{i_1 i_2}(\omega) + \frac{e}{i\hbar} A_R(\omega) \sum_{i_3} (V_{i_2 i_3} n^0_{i_1 i_3} - V_{i_3 i_1} n^0_{i_3 i_2}) + \sum_{i_3, i_4, i_5} (-\Gamma^{\text{out}}_{i_2 i_3 i_4 i_5} \{\Delta n_{i_1 i_5}(\omega) \delta_{i_4, i_3} - \alpha_B [n^0_{i_1 i_5} \Delta n_{i_4 i_3}(\omega)$$

$$+ n^0_{i_4 i_3} \Delta n_{i_1 i_5}(\omega)]\} - \Gamma^{\text{out}*}_{i_1 i_3 i_4 i_5} \{\Delta n_{i_5 i_2}(\omega) \delta_{i_3, i_4} - \alpha_B [n^0_{i_5 i_2} \Delta n_{i_3 i_4}(\omega) + n^0_{i_3 i_4} \Delta n_{i_5 i_2}(\omega)]\} + \Gamma^{\text{in}}_{i_2 i_3 i_4 i_5} \{\Delta n_{i_4 i_3}(\omega) \delta_{i_1, i_5}$$

$$- \alpha_B [n^0_{i_1 i_5} \Delta n_{i_4 i_3}(\omega) + n^0_{i_4 i_3} \Delta n_{i_1 i_5}(\omega)]\} + \Gamma^{\text{in}*}_{i_1 i_3 i_4 i_5} \{\Delta n_{i_3 i_4}(\omega) \delta_{i_5, i_2} - \alpha_B [n^0_{i_5 i_2} \Delta n_{i_3 i_4}(\omega) + n^0_{i_3 i_4} \Delta n_{i_5 i_2}(\omega)]\}). \quad (30)$$

Current density in the frequency domain in both the non-Markovian and Markovian descriptions may be obtained from

$$\Delta J(\omega) = -\frac{e}{d} \left[\sum_{i_1=1}^{N} \frac{1}{m^*} e A_R(\omega) n^0_{i_1 i_1} + \sum_{i_1, i_2=1}^{N} \left(\frac{i}{\hbar} (E_{i_1} - E_{i_2}) z_{i_1 i_2} \Delta n_{i_2 i_1}(\omega) + \frac{i}{\hbar} (E_{i_1} - E_{i_2+N}) z_{i_1 (i_2+N)} \Delta n_{(i_2+N) i_1}(\omega) \right. \right.$$

$$\left. \left. + \frac{i}{\hbar} (E_{i_2+N} - E_{i_1}) z_{i_1 (i_2+N)} \Delta n_{i_1 (i_2+N)}(\omega) \right) \right]. \quad (31)$$

In the Boltzmann description, the gain coefficient may be written as

$$g(\omega) = \frac{\pi e^2}{n \epsilon_0 c \omega \hbar^2 d} \sum_{i,f=1}^{N} n_i [(E_i - E_f)^2 \, \text{sgn}(E_i - E_f) z^2_{m_i, m_f} \delta(|E_i - E_f| - \hbar\omega) + (E_i - E_{f+N})^2 \, \text{sgn}(E_i - E_{f+N}) z^2_{m_i, m_{f+N}}$$

$$\times \delta(|E_i - E_{f+N}| - \hbar\omega) + (E_{i+N} - E_f)^2 \, \text{sgn}(E_{i+N} - E_f) z^2_{m_{i+N}, m_f} \delta(|E_{i+N} - E_f| - \hbar\omega)]. \quad (32)$$

The δ function in the gain coefficient expression is modeled by a Lorentzian with the same FWHM as for electron-LO phonon scattering rates.

III. NUMERICAL RESULTS AND DISCUSSION

As a prototypical system, we consider a QCL design which comprises a three-level scheme, and employs LO-phonon depopulation of the lower laser level to the ground state. No injector region is present and efficient injection into the upper laser level is enabled by its alignment with the ground level of the preceding period. The QCL period consists of two QWs (see Fig. 1), one of which confines the ground and lower laser levels, whose energy difference is set to be approximately one LO phonon energy (36.9 meV). The upper laser level is localized in the other well. This structure was chosen to be examined, instead of existing QCLs already investigated in the presence of a magnetic field, due to its simplicity, and the dominant influence of the electron-LO phonon interaction on the electron population dynamics, as will be explained in what follows.

The conduction band profile and electronic structure of the QCL in zero magnetic field and an electric field of 16.2 kV/cm, are given in Fig. 1. One QCL period includes a 2.8 nm $Al_{0.3}Ga_{0.7}As$ barrier, followed by a 9 nm GaAs well,

a 1.4 nm $Al_{0.3}Ga_{0.7}As$ barrier, and a 17.4 nm GaAs well. States 1, 2, and 3 represent the ground, lower laser, and upper laser levels, respectively, and states 1′ and 3″ represent the ground level of the preceding period and the upper laser level of the following period. The doping density was chosen
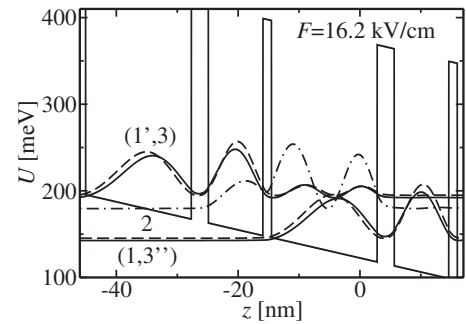

FIG. 1. A schematic diagram of the conduction band profile, size-quantized energy levels from which Landau levels originate, and squared wave functions for one full period and parts of adjacent periods of the GaAs/AlGaAs QCL for zero magnetic field, and an electric field of 16.2 kV/cm. States 1 and 1′ (solid line), 2 (dashed-dotted line), 3 and 3″ (dashed line) denote the ground, lower laser, and upper laser levels, respectively. State 1′ belongs to the preceding period, while state 3″ belongs to the following period.
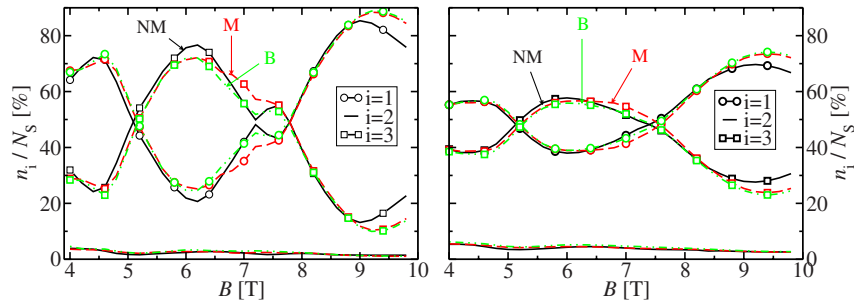
FIG. 2. (Color online) The electron population over QCL states (all Landau levels) vs magnetic field. States 1, 2, and 3 represent the ground state, the lower laser level, and the upper laser level, respectively. N_S is the total sheet density of electrons per period. Solid, dashed, and dashed-double-dotted lines represent non-Markovian (NM), Markovian (M), and Boltzmann (B) results, respectively. Left-hand side, $\hbar\gamma = 1$ meV. Right-hand side, $\hbar\gamma = 2$ meV.

to be 10^{11} cm^{-2}, in order to achieve relatively high gain in the THz range, while still having a small influence on the effective conduction band potential and making electron-electron processes less relevant. The temperature was set to 4 K, since QCLs in a magnetic field are usually operated at low temperatures. The transition energy between the upper and lower laser levels is 15.2 meV, and the energy difference between the ground state and the upper laser level of the following period is 2.6 meV.

Relatively strong electron-electron scattering occurs between the ground state and the upper laser level of the next period, due to a large overlap and small energy difference. However, the semiclassical calculation performed for a similar structure showed that the electron-LO phonon scattering rates from the lower laser level to these levels, also relevant for the distribution of electrons between them, are considerably larger.[42] Electron-electron processes between other states are less important, due to the large energy spacing of significantly populated LLs. Consequently, we expect that the population dynamics are not significantly influenced by electron-electron scattering. We make an assumption that the same accounts for the polarization dynamics and as is usual with quantum-mechanical models of transport in QCLs[11-13] we neglect electron-electron scattering hereafter.

A. Electron populations

The populations of all LLs associated with the ground state and the upper and lower laser levels, calculated using the non-Markovian, Markovian, and Boltzmann model of electron transport, as functions of magnetic field, are shown in Fig. 2. In the calculation, we used the values of the damping parameter of $\hbar\gamma = 1$ meV and $\hbar\gamma = 2$ meV. Regardless of the model used, the dependencies of the populations on the magnetic field are generally similar. For some values of the magnetic field (4.6 T, 9.2 T), the energy difference between some LLs stemming from the upper laser level and the ground state becomes equal to one LO phonon energy, thus the electron-LO phonon interaction between them increases considerably. Consequently, the population of all LLs stemming from the upper laser level decreases reaching its minimum, while the opposite happens to the population of the

LLs stemming from the ground state. Conversely, for intermediate magnetic fields (6.2 T), the population of the upper laser level is increased, while the ground state is depopulated. The population of the lower laser level practically does not change with magnetic field.

The populations obtained from the Markovian and Boltzmann description do not differ much, except in the range of magnetic fields between 6.2 T and 8 T, see Fig. 2. In the fully nondiagonal Markovian (and non-Markovian) approach employed here, the coupling between populations and polarizations is accounted for, which results in the presence of phase coherence in the stationary state. In other words, during the time evolution of the system, scattering processes from populations to polarizations create an amount of polarization in steady-state conditions. These and reverse processes (dephasing from polarizations to populations) may have an observable impact on electron populations. More pronounced differences between the Markovian and Boltzmann populations, for magnetic fields between 6.2 T and 8 T, indicate a stronger interplay between populations and polarizations in the Markovian description and, hence, larger values of polarizations. Indeed, Figs. 3 and 4 show that the polarizations between all LLs stemming from any two laser states are increased for these magnetic fields.
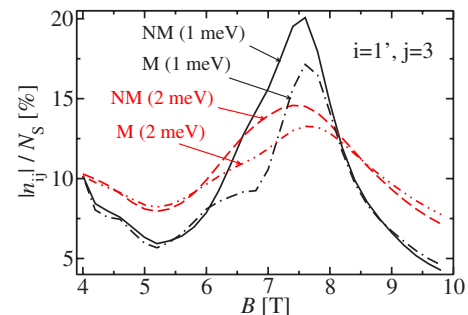

FIG. 3. (Color online) The electron polarization between the ground state of the preceding period and the upper laser level (all Landau levels) vs magnetic field. N_S is the total sheet density of electrons per period. Solid, dashed, dashed-dotted, and dashed-double-dotted lines represent non-Markovian (NM) ($\hbar\gamma = 1$ meV and $\hbar\gamma = 2$ meV) and Markovian (M) results, respectively.
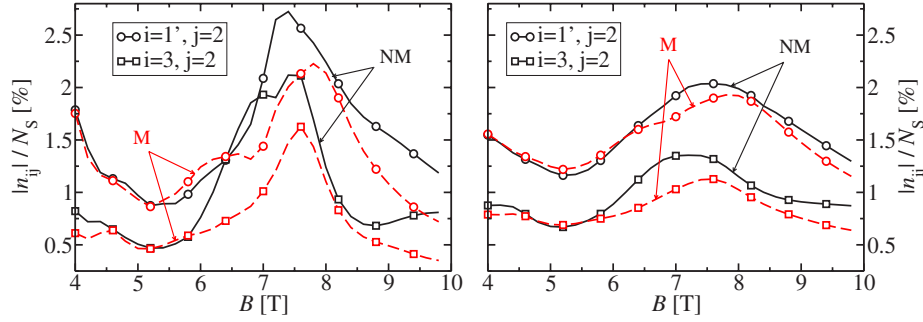
FIG. 4. (Color online) The electron polarization between the lower laser level and other QCL states (all Landau levels) vs magnetic field. States 1′, 2, and 3 represent the ground state of the preceding period, the lower laser level, and the upper laser level, respectively. N_S is the total sheet density of electrons per period. Solid and dashed lines represent non-Markovian (NM) and Markovian (M) results, respectively. Left-hand side, $\hbar\gamma=1$ meV. Right-hand side, $\hbar\gamma=2$ meV.

The Markovian and Boltzmann calculations for different values of the damping parameter γ showed that the LL populations are very similar to the corresponding quantum-kinetic results, see Fig. 2. Nevertheless, this does not mean that there is one-to-one correspondence between these electron transport models. The non-Markovian description accounts for the memory of scattering and dephasing processes, which corresponds to a quantum-mechanical energy-time uncertainty. In comparison, the Markovian or Boltzmann dynamics take into account only energy-conserving processes, here, however, relaxed by the assumption that all LLs are broadened. This may lead to different values of polarizations, gain, and current although the populations are quite similar.

B. Electron polarizations

Figures 3 and 4 show the most prominent polarizations between all LLs associated with pairs of laser states, obtained from the Markovian and non-Markovian models ($\hbar\gamma=1$ meV and $\hbar\gamma=2$ meV), as they depend on the magnetic field. In all cases, the polarization between the ground state and the upper laser level of the next period, shown in Fig. 3, is considerable ($\sim 10\%$), due to the fact that these levels actually constitute a doublet state. Although their overlap does not change with magnetic field, their polarization does, since the LL electronic structure and all scattering and/or

dephasing processes change as well. The polarizations between the upper laser level or the ground state of the previous period and the lower laser level are an order of magnitude smaller ($\sim 1\%$), see Fig. 4. This rapidly decreasing trend continues for the polarizations between other pairs of states, due to strong electron-LO phonon dephasing.

Generally, nondiagonal contribution curves in each Markovian case are offset to smaller values compared to the corresponding non-Markovian ones. This is caused by smaller scattering rates from populations to polarizations in the Markovian case, since they do not include the memory of the interaction. The coherences in the Markovian case for $\hbar\gamma=1$ meV have larger peaks than for $\hbar\gamma=2$ meV, while away from the peak, their values become smaller. The effect of smaller broadening is that the scattering rates responsible for the formation of polarizations have larger peak and lower valley values. The same conclusion applies to the non-Markovian results. To illustrate this, the most influential scattering rates from populations to the polarization between the states of the doublet in the Markovian case versus magnetic field are shown in Fig. 5. The average scattering rate from the polarizations between LLs originating from state m_{i_1} and m_{i_2} into the polarizations between LLs originating from states m_{i_4} and m_{i_3} may be defined in the Markovian approach according to
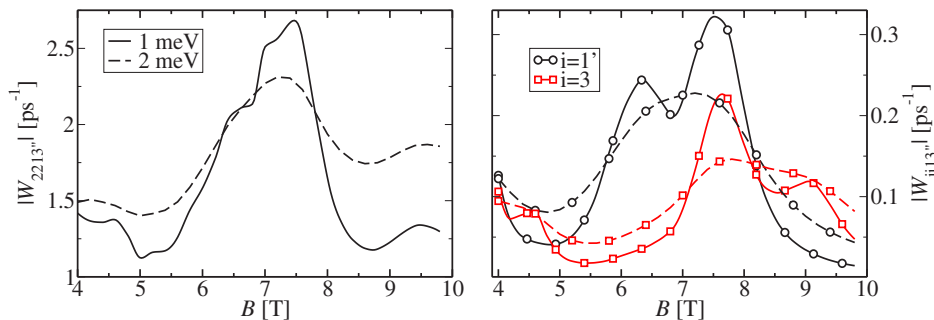

FIG. 5. (Color online) Average scattering rates (see text for explanation) from QCL states to polarizations between QCL states vs magnetic field, calculated in the Markovian approach for $\hbar\gamma=1$ meV (solid lines) and $\hbar\gamma=2$ meV (dashed lines). States 1, 2, and 3 represent the ground state, the lower laser level, and the upper laser level, respectively. States 1′ and 3″ denote the ground state of the preceding period, and the upper laser level of the following period.

$$W^a_{m_{i_1}m_{i_2}m_{i_3}m_{i_4}} = \sum_{m_{i_5}} \sum_{j_{i_1} - j_{i_5}} n_{|m_{i_1},j_{i_1}\rangle,|m_{i_5},j_{i_5}\rangle} \Gamma^{out}_{|m_{i_2},j_{i_2}\rangle,|m_{i_3},j_{i_3}\rangle,|m_{i_4},j_{i_4}\rangle,|m_{i_5},j_{i_5}\rangle} \frac{(\delta_{|m_{i_4},j_{i_4}\rangle,|m_{i_3},j_{i_3}\rangle} - \alpha_B n_{|m_{i_4},j_{i_4}\rangle|m_{i_3},j_{i_3}\rangle})}{\sum_{m_{i_5}} \sum_{j_{i_1},j_{i_5}} n_{|m_{i_1},j_{i_1}\rangle,|m_{i_5},j_{i_5}\rangle}}$$

$$+ \sum_{m_{i_5}} \sum_{j_{i_1} - j_{i_5}} n_{|m_{i_5},j_{i_5}\rangle|m_{i_2},j_{i_2}\rangle} \Gamma^{out*}_{|m_{i_1},j_{i_1}\rangle,|m_{i_4},j_{i_4}\rangle,|m_{i_3},j_{i_3}\rangle,|m_{i_5},j_{i_5}\rangle} \frac{(\delta_{|m_{i_4},j_{i_4}\rangle,|m_{i_3},j_{i_3}\rangle} - \alpha_B n_{|m_{i_4},j_{i_4}\rangle|m_{i_3},j_{i_3}\rangle})}{\sum_{m_{i_5}} \sum_{j_{i_1},j_{i_5}} n_{|m_{i_5},j_{i_5}\rangle,|m_{i_2},j_{i_2}\rangle}}. \qquad (33)$$

Under the condition that $m_{i_1} = m_{i_2}$, Eq. (33) gives the average scattering rate from LLs associated with state m_{i_1} into the polarizations between LLs associated with states m_{i_4} and m_{i_3}. Also, the condition $m_{i_1} = m_{i_2}$ and $m_{i_3} = m_{i_4}$ gives the average scattering rate from LLs stemming from state m_{i_1} into LLs stemming from state m_{i_3}, which is equivalent to the Boltzmann scattering rate.

C. Optical gain

In addition to direct transitions of electrons between two energy states due to emission or absorption of photons [the first equation in Eq. (29)], the non-Markovian approach also accounts for transitions between these states involving emission or absorption of both photons and LO phonons [see the denominator in the second equation in Eq. (29)]. Since the latter include an additional influence of LO phonons, it is reasonable to expect that the linewidth of LO phonon-assisted optical transitions is wider in comparison to the one of direct optical transitions. Indeed, for photon energies $\hbar\omega$ which correspond to resonant LO phonon-assisted optical transitions, the gain and/or absorption linewidth is of the order of $2\hbar\gamma$ [see the second equation in Eq. (29)]. On the other hand, when discussing resonant direct optical transitions, we should note that their dynamics are coupled with the dynamics of LO phonon-assisted transitions. Formally, the latter may be interpreted as some kind of scattering processes, which do not yield energy conservation, but include an additional $\hbar\omega$ contribution.[41] Therefore, the gain linewidth of direct transitions is determined by these "scattering processes," whose intensity is strongly influenced by the energy spectra of the system. If resonant LO phonon-assisted transitions do not occur for the same photon energies as direct ones, all "scattering rates" are significantly smaller than in the resonant case, and so is the linewidth. In the Markov-

ian description, only direct optical transitions are taken into account [see Eq. (30)], whose linewidth is determined by the energy conserving scattering processes, which are strongly dependent on the inter-LL separation. In the Boltzmann approach, the broadening due to the interaction of electrons with light is taken to be equal to the broadening due to the interaction of electrons with LO phonons, consequently, the linewidth of direct optical transitions is given with $2\hbar\gamma$.

The gain spectra for a magnetic field of 4 T in the energy range close to the laser transition energies and one LO phonon energy, are shown in Figs. 6 and 7, respectively. The gain coefficient was calculated for the non-Markovian, Markovian, and Boltzmann dynamics ($\hbar\gamma = 1$ meV and $\hbar\gamma = 2$ meV). In the case of resonant direct optical transitions between either the upper laser level or the ground state of the previous period and the lower laser level ($\hbar\omega \approx \bar{E}_3 - \bar{E}_2$ or $\hbar\omega \approx \bar{E}_{1'} - \bar{E}_2$, respectively), there is no additional contribution of resonant LO phonon-assisted optical transitions for the QCL considered. In contrast, for photon energies close to one LO phonon energy, such contributions do appear, and are related to absorption of photons followed by emission of phonons with no electron transitions involved or with electron transitions between energetically close states (the upper laser level and the ground state of the previous period). Consequently, the gain linewidth for the energies corresponding to the laser transitions is considerably smaller than for the energies around one LO phonon energy, compare Figs. 6 and 7. However, in a real QCL device, it is likely that the interaction of electrons with impurities, interface defects, and other electrons, as well as imperfect periodicity, will broaden the LLs making the gain linewidth for laser transition energies not as narrow as the non-Markovian model predicts.

In the Markovian description, since the LO phonon resonances between the lower laser level and either the ground state or the upper laser level of the next period are present in
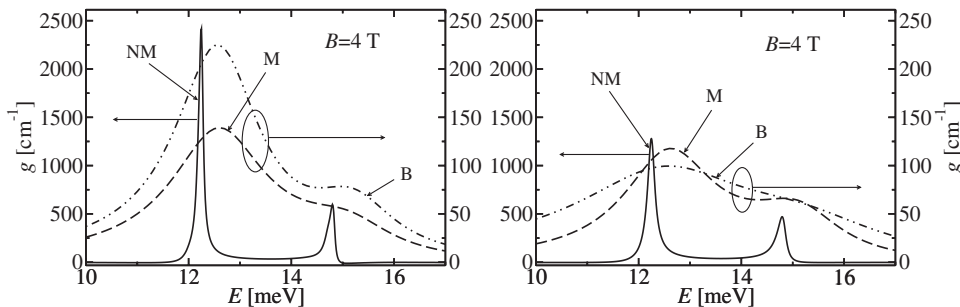

FIG. 6. Optical gain vs energy for a magnetic field of 4 T. The energy range is in the vicinity of the laser transition energies. Solid, dashed, and dashed-double-dotted lines represent non-Markovian (NM), Markovian (M), and Boltzmann (B) results, respectively. Left-hand side, $\hbar\gamma = 1$ meV. Right-hand side, $\hbar\gamma = 2$ meV.
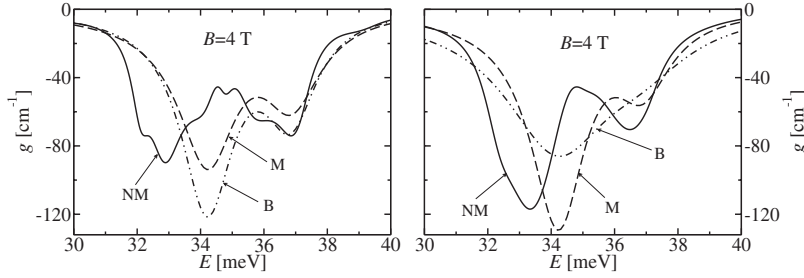
FIG. 7. Optical gain vs energy for a magnetic field of 4 T. The energy range is in the vicinity of one longitudinal optical phonon energy. Solid, dashed, and dashed-double-dotted lines represent non-Markovian (NM), Markovian (M), and Boltzmann (B) results, respectively. Left-hand side, $\hbar\gamma=1$ meV. Right-hand side, $\hbar\gamma=2$ meV.

the energy spectra, the corresponding resonant scattering terms lead to large linewidths of gain features throughout the frequency range of interest (considerably larger than the non-Markovian linewidth for the laser transition energies and comparable to the non-Markovian linewidth for energies close to one LO phonon energy). We should note that, if there were no such LO phonon resonances in the system, the gain linewidth in the Markovian description would be smaller. As a consequence, we observe a significant difference between the Markovian and non-Markovian gain linewidth for the laser transition energies. A similar result for direct optical transitions at low temperatures in quantum wells without magnetic field has also been reported in Ref. 18.

In the Markovian limit, energy renormalizations, describing the polaron corrections to the band structure, are ignored. However, the polaron shift is always included in the quantum-kinetic treatment. It is more prominent for the energy transitions close to one LO phonon energy (~ 1 meV), but it is also present for the laser transition energies (~ 0.4 meV).

Figure 8 illustrates the gain profile for a magnetic field of 6 T in the energy range around the laser transition energies and one LO phonon energy, calculated from the non-Markovian model for $\hbar\gamma=1$ meV and $\hbar\gamma=2$ meV. Comparison of the non-Markovian gain spectra for different values of the damping parameter (see also Figs. 6 and 7) reveals pronounced differences between both the gain linewidth and peak values. Sensitivity of the results to the values of the phenomenological parameter confirms the need for a self-consistent incorporation of higher-order correlations in the quantum-kinetic model, which would require a significant

increase in computational time. Moreover, for a magnetic field of 6 T, apart from the two expected peaks associated with the transitions from the lower laser level to the ground state or the upper laser level of the subsequent period, which are in the vicinity of one LO phonon energy, an extra peak at $\hbar\omega=34.3$ meV appears for $\hbar\gamma=1$ meV, in comparison to $\hbar\gamma=2$ meV, see Fig. 8. This is due to the fact that, for the electronic structure of the QCL considered, peaks due to resonant LO phonon-assisted optical transitions may also emerge in that energy range. Careful inspection of Eq. (29) reveals the presence of resonances at the energies of $\hbar\omega \approx \pm (E_{|3''j\rangle}-E_{|1,j\rangle})+\hbar\omega_{LO}=\pm 2.6$ meV$+\hbar\omega_{LO}$, as discussed earlier. At first, it may appear that one of these resonances, related to the transition between the ground state and the upper laser level of the subsequent period, is manifested via that additional peak in the gain and/or absorption spectra (a so-called polaron satellite).[18] However, this is not entirely the case here. Due to a nontrivial interplay between these resonant LO phonon-assisted terms, and resonant direct optical transitions from the lower laser level to the ground state or the upper laser level of the following period which occur at similar energies, $\Delta n_{|1,j\rangle|2,j\rangle}(\omega)$ or $\Delta n_{|3'',j\rangle|2,j\rangle}(\omega)$ constitute a much larger fraction of the total gain for energies close to $\hbar\omega_{LO}$ than $\Delta n_{|3'',j\rangle|1,j\rangle}(\omega)$. Here, the peak at $\hbar\omega=34.3$ meV for $B=6$ T and $\hbar\gamma=1$ meV is actually related to the transition between the lower laser level and the upper laser level of the next period [the calculation showed that $\Delta n_{|1,j\rangle|2,j\rangle}(\omega) < \Delta n_{|3'',j\rangle|2,j\rangle}(\omega)$], as well as the peak at $\hbar\omega=32.7$ meV which is also present for $\hbar\gamma=2$ meV, while the peak at $\hbar\omega=36.8$ meV is associated with the transition between the lower laser level and the ground state. In fact, the previous analysis of the terms which are resonant for the energies in
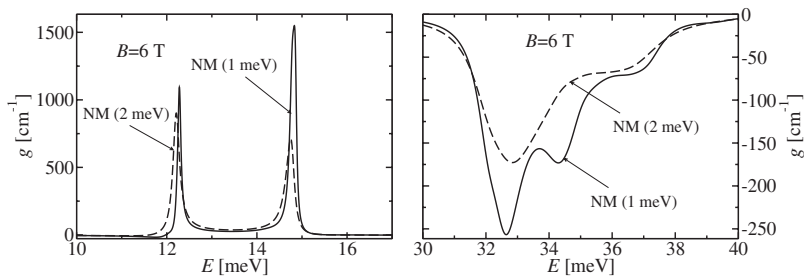

FIG. 8. Optical gain vs energy for a magnetic field of 6 T calculated using the non-Markovian (NM) approach for $\hbar\gamma=1$ meV (solid line) and $\hbar\gamma=2$ meV (dashed line). Left-hand side, the energy range is in the vicinity of the laser transition energies. Right-hand side, the energy range is in the vicinity of one longitudinal optical phonon energy.
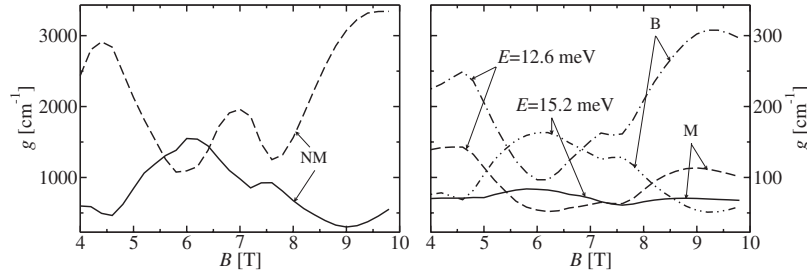
FIG. 9. Maximal gain vs magnetic field for transitions from the upper laser level and the ground state of the preceding period to the lower laser level for $\hbar\gamma = 1$ meV. Left-hand side, the non-Markovian (NM) results are represented by solid and dashed lines, respectively. Right-hand side, the Markovian (M) results are represented by solid and dashed lines, respectively. The Boltzmann (B) results are represented by dashed-dotted and dashed-double-dotted lines, respectively.

the vicinity of one LO phonon energy suggests that several peaks could emerge in the absorption spectra in that energy range. Due to their proximity, some of them may be obscured by other stronger peaks for different values of the damping parameter and magnetic fields. In Fig. 7, for the value of the damping parameter of $\hbar\gamma = 1$ meV, we can see that, in addition to two well-defined peaks, four small ones also appear.

Figure 9 shows the peak gain versus magnetic field dependence, for transitions from the upper laser level and the ground level of the preceding period to the lower laser level, obtained from the non-Markovian, Markovian, and Boltzmann ($\hbar\gamma = 1$ meV) approach. The general trend of the non-Markovian gain is fairly similar to the Markovian or Boltzmann results, although the former has larger values. The oscillations of the gain in both types of transitions reproduce reasonably well the oscillations of the related populations (see Fig. 2). It should be noted that, for most magnetic fields, the dominant gain spectral component is not generated in the transitions from the upper laser level, but from the ground state of the preceding period, even at some magnetic fields for which the upper laser level is more populated. The reason for that is a slightly larger dipole matrix element between the ground state of the preceding period and the lower laser level.

D. Current

The current densities as functions of magnetic field, calculated using the non-Markovian, Markovian, and Boltzmann description ($\hbar\gamma = 1$ meV and $\hbar\gamma = 2$ meV), are shown in Fig. 10. From Eq. (23), used in the Markovian and non-Markovian approach, it follows that diagonal density matrix elements do not contribute to the total current.[9,13] Therefore, the electron transport is entirely due to nondiagonal density matrix contributions, i.e., scattering induced phase coher-

ences between the laser states. This quantum-mechanical picture of completely coherent current is in a stark contrast with the semiclassical picture of transport through scattering transitions. However, both descriptions give similar results, see Fig. 10. Here, the nondiagonal density matrix element are considerably smaller in comparison to the diagonal ones (see Figs. 2–4), thus the former may be approximated in terms of the latter,[13,40] giving Eq. (24) used in the calculation of the semiclassical current, and resulting in comparable values of the current density.

In the semiclassical interpretation, the electron transport channel from one doublet directly to the subsequent doublet is as important as the channel which additionally involves the lower laser level. The scattering rates from the lower laser level to the ground state and the upper laser level of the next period do not exhibit pronounced oscillations with magnetic field since those energy transitions are close to one LO phonon energy. Therefore, the current versus magnetic field dependence in the semiclassical picture is mainly determined by the scattering rates between the doublet states, shown in Fig. 11, and their populations. In the Markovian and non-Markovian description, the current is completely determined by the polarizations between the QCL states, see the diagrams shown in Figs. 3, 4, and 10. In both approaches, the current density curves reproduce well the main features of the related polarization curves. Also, the discrepancies between the current densities estimated from the Markovian and non-Markovian treatments are identical to those between the related polarizations.

IV. CONCLUSION

We have presented a quantum kinetic description of electron dynamics and gain in QCLs subjected to a magnetic
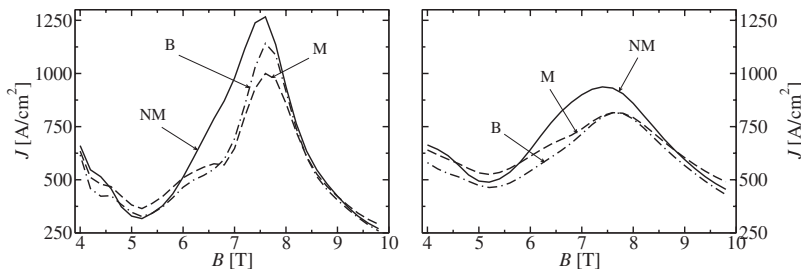

FIG. 10. Current density vs magnetic field dependence. Solid, dashed, and dashed-dotted lines represent non-Markovian (NM), Markovian (M), and Boltzmann (B) results, respectively. Left-hand side, $\hbar\gamma = 1$ meV. Right-hand side, $\hbar\gamma = 2$ meV.
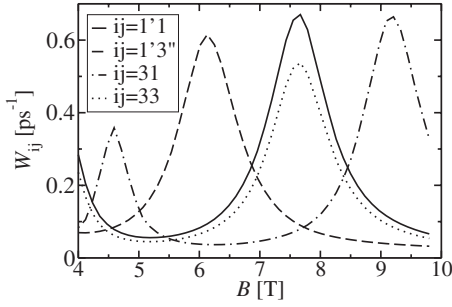
FIG. 11. Average scattering rates (see text for explanation) between QCL states vs magnetic field, calculated in the Boltzmann description for $\hbar\gamma = 1$ meV. States 1, 2, and 3 represent the ground state, the lower laser level, and the upper laser level, respectively. States $1'$ and $3''$ denote the ground state of the preceding period and the upper laser level of the following period.

field based on the density matrix formalism. As a first step, electron-LO phonon interaction was considered as the most relevant scattering and/or dephasing mechanism. Nonequilibrium stationary state populations and polarizations for an example of the QCL structure were calculated using various kinetic models (non-Markovian, Markovian, and Boltzmann). We showed that steady-state populations in all of these models are similar for a range of magnetic fields, and then we compared other relevant quantities (polarizations,

gain, current). In both the Markovian and non-Markovian approach, coherent polarizations induced by electron-LO phonon interaction were found to be relatively small. This in turn led to similar values of the entirely coherent current in the Markovian and non-Markovian picture compared to the values of the entirely incoherent current in the Boltzmann interpretation. Gain spectra in the non-Markovian treatment showed considerably narrow linewidths for laser transitions and evidence of polaron formation, in contrast to the Markovian and Boltzmann predictions.

ACKNOWLEDGMENTS

APPENDIX A

This appendix presents a detailed derivation of the quantum kinetic equations for electron populations and polarizations in QWs under an applied magnetic field. The procedure for obtaining appropriate expressions in the Markovian approximation is also given.

Equations (11) and (15) represent a starting point for the derivation of the quantum kinetic equations of motion, giving the following expressions

$$
\frac{d}{dt}\delta s^{i_1 i_2}_{k,\mathbf{q},k-q_y} = \frac{1}{i\hbar}(E_{i_2} + \hbar\omega_{\mathrm{LO}} - E_{i_1})\delta s^{i_1 i_2}_{k,\mathbf{q},k-q_y} - \gamma\delta s^{i_1 i_2}_{k,\mathbf{q},k-q_y} + \frac{1}{i\hbar}\sum_{i_4,i_5} g^*_{\mathbf{q}}H^*_{j_{i_5}j_{i_4}}(k, k-q_y, q_x)
$$
$$
\times G^*_{m_{i_5}m_{i_4}}(q_z)[(n_0+1)f_{i_1 i_5,k}(\delta_{i_4,i_2} - f_{i_4 i_2, k-q_y}) - n_0 f_{i_4 i_2, k-q_y}(\delta_{i_1,i_5} - f_{i_1 i_5,k})],
$$

$$
\frac{d}{dt}f_{i_1 i_2,k}\bigg|_{\hat{H}_{ep}} = \frac{1}{i\hbar}\sum_{i_3,\mathbf{q}}[g_{\mathbf{q}}H_{j_{i_2}j_{i_3}}(k, k-q_y, q_x)G_{m_{i_2}m_{i_3}}(q_z)\delta s^{i_1 i_3}_{k,\mathbf{q},k-q_y} + g^*_{\mathbf{q}}H^*_{j_{i_3}j_{i_2}}(k+q_y, k, q_x)G^*_{m_{i_3}m_{i_2}}(q_z)\delta s^{i_3 i_1 *}_{k+q_y,\mathbf{q},k}
$$
$$
- g_{\mathbf{q}}H_{j_{i_3}j_{i_1}}(k+q_y, k, q_x)G_{m_{i_3}m_{i_1}}(q_z)\delta s^{i_3 i_2}_{k+q_y,\mathbf{q},k} - g^*_{\mathbf{q}}H^*_{j_{i_1}j_{i_3}}(k, k-q_y, q_x)G^*_{m_{i_1}m_{i_3}}(q_z)\delta s^{i_2 i_3 *}_{k,\mathbf{q},k-q_y}]. \tag{A1}
$$

The assumption of an initially uncorrelated system $[\lim_{t\to -\infty}\delta s^{i_1 i_2}_{k,\mathbf{q},k-q_y}(t) = 0]$ gives

$$
\delta s^{i_1 i_2}_{k,\mathbf{q},k-q_y} = \frac{1}{i\hbar}\sum_{i_4,i_5} g^*_{\mathbf{q}}H^*_{j_{i_5}j_{i_4}}(k, k-q_y, q_x)G^*_{m_{i_5}m_{i_4}}(q_z)\int_{-\infty}^{t} dt' \exp\left[\left(\frac{1}{i\hbar}(E_{i_2} + \hbar\omega_{\mathrm{LO}} - E_{i_1}) - \gamma\right)(t-t')\right]
$$
$$
\times[(n_0+1)f_{i_1 i_5,k}(\delta_{i_4,i_2} - f_{i_4 i_2, k-q_y}) - n_0 f_{i_4 i_2, k-q_y}(\delta_{i_1,i_5} - f_{i_1 i_5,k})]
$$
$$
= \sum_{i_4,i_5} g^*_{\mathbf{q}}H^*_{j_{i_5}j_{i_4}}(k, k-q_y, q_x)G^*_{m_{i_5}m_{i_4}}(q_z)\delta K^{i_1 i_2 i_4 i_5}_{k,\mathbf{q},k-q_y}, \tag{A2}
$$

where the quantities $\delta K^{i_1 i_2 i_4 i_5}_{k,\mathbf{q},k-q_y}$ related to the phonon-assisted matrices $\delta s^{i_1 i_2}_{k,\mathbf{q},k-q_y}$ are represented as

$$
\frac{d}{dt}\delta K^{i_1 i_2 i_4 i_5}_{k,\mathbf{q},k-q_y} = \frac{1}{i\hbar}(E_{i_2} + \hbar\omega_{\mathrm{LO}} - E_{i_1})\delta K^{i_1 i_2 i_4 i_5}_{k,\mathbf{q},k-q_y} - \gamma\delta K^{i_1 i_2 i_4 i_5}_{k,\mathbf{q},k-q_y} + \frac{1}{i\hbar}[(n_0+1)f_{i_1 i_5,k}(\delta_{i_4,i_2} - f_{i_4 i_2, k-q_y}) - n_0 f_{i_4 i_2, k-q_y}(\delta_{i_1,i_5} - f_{i_1 i_5,k})].
$$
$$
\tag{A3}
$$

Simple algebra then leads to equations for the dynamics of populations and polarizations in the form

$$\frac{d}{dt}f_{i_1i_2,k}\bigg|_{\hat{H}_{ep}} = \frac{1}{i\hbar}\sum_{i_3,i_4,i_5,\mathbf{q}}|g_{\mathbf{q}}|^2 \times [H_{j_{i_2}j_{i_3}}(k,k-q_y,q_x)H^*_{j_{i_5}j_{i_4}}(k,k-q_y,q_x)G_{m_{i_2}m_{i_3}}(q_z)G^*_{m_{i_5}m_{i_4}}(q_z)\delta K^{i_1i_3i_4i_5}_{k,\mathbf{q},k-q_y} + H^*_{j_{i_3}j_{i_2}}(k+q_y,k,q_x)$$

$$\times H_{j_{i_4}j_{i_5}}(k+q_y,k,q_x)G^*_{m_{i_3}m_{i_2}}(q_z)G_{m_{i_4}m_{i_5}}(q_z)\delta K^{i_3i_1i_5i_4*}_{k+q_y,\mathbf{q},k} - H_{j_{i_3}j_{i_1}}(k+q_y,k,q_x)H^*_{j_{i_4}j_{i_5}}(k+q_y,k,q_x)G_{m_{i_3}m_{i_1}}(q_z)$$

$$\times G^*_{m_{i_4}m_{i_5}}(q_z)\delta K^{i_3i_2i_5i_4}_{k+q_y,\mathbf{q},k} - H^*_{j_{i_1}j_{i_3}}(k,k-q_y,q_x)H_{j_{i_5}j_{i_4}}(k,k-q_y,q_x)G^*_{m_{i_1}m_{i_3}}(q_z)G_{m_{i_5}m_{i_4}}(q_z)\delta K^{i_2i_3i_4i_5*}_{k,\mathbf{q},k-q_y}]. \tag{A4}$$

From the expression for the lateral overlap integrals derived in Appendix B [Eqs. (B7) and (B9)], the following expressions can be shown:

$$H_{j_{i_1}j_{i_3}}(k,k-q_y,q_x)H^*_{j_{i_5}j_{i_4}}(k,k-q_y,q_x) = |H_{j_{i_1}j_{i_3}}(q_{xy})||H_{j_{i_5}j_{i_4}}(q_{xy})|e^{i(\pi/2)a_1}e^{i\theta(j_{i_1}+j_{i_4}-j_{i_3}-j_{i_5})},$$

$$H^*_{j_{i_3}j_{i_1}}(k+q_y,k,q_x)H_{j_{i_4}j_{i_5}}(k+q_y,k,q_x) = |H_{j_{i_3}j_{i_1}}(q_{xy})||H_{j_{i_4}j_{i_5}}(q_{xy})|e^{i(\pi/2)a_1}e^{i\theta(j_{i_1}+j_{i_4}-j_{i_3}-j_{i_5})}, \tag{A5}$$

where $\theta=\arg(q_x+iq_y)$ and

$$a_1 = \begin{cases} j_{i_1} + j_{i_4} - j_{i_3} - j_{i_5}, & j_{i_1} > j_{i_3} \wedge j_{i_5} > j_{i_4}, \\ -j_{i_1} - j_{i_4} + j_{i_3} + j_{i_5}, & j_{i_1} < j_{i_3} \wedge j_{i_5} < j_{i_4}, \\ j_{i_1} - j_{i_4} - j_{i_3} + j_{i_5}, & j_{i_1} > j_{i_3} \wedge j_{i_5} < j_{i_4}, \\ -j_{i_1} + j_{i_4} + j_{i_3} - j_{i_5}, & j_{i_1} < j_{i_3} \wedge j_{i_5} > j_{i_4}, \end{cases}$$

hold. Then, the temporal evolution of the density matrix elements read as follows:

$$\frac{d}{dt}f_{i_1i_2,k}\bigg|_{\hat{H}_{ep}} = \frac{1}{i\hbar}\sum_{i_3,i_4,i_5,\mathbf{q}}|g_{\mathbf{q}}|^2 \times [H_{j_{i_2}j_{i_3}}(q_{xy})||H_{j_{i_5}j_{i_4}}(q_{xy})|G_{m_{i_2}m_{i_3}}(q_z)G^*_{m_{i_5}m_{i_4}}(q_z)e^{i(\pi/2)a_2}e^{i\theta(j_{i_2}+j_{i_4}-j_{i_3}-j_{i_5})}\delta K^{i_1i_3i_4i_5}_{k,\mathbf{q},k-q_y}$$

$$+ |H_{j_{i_3}j_{i_2}}(q_{xy})||H_{j_{i_4}j_{i_5}}(q_{xy})|G^*_{m_{i_3}m_{i_2}}(q_z)G_{m_{i_4}m_{i_5}}(q_z)e^{i(\pi/2)a_2}e^{i\theta(j_{i_2}+j_{i_4}-j_{i_3}-j_{i_5})}\delta K^{i_3i_1i_5i_4*}_{k+q_y,\mathbf{q},k}$$

$$- |H_{j_{i_3}j_{i_1}}(q_{xy})||H_{j_{i_4}j_{i_5}}(q_{xy})|G_{m_{i_3}m_{i_1}}(q_z)G^*_{m_{i_4}m_{i_5}}(q_z)e^{-i(\pi/2)a_1}e^{-i\theta(j_{i_1}+j_{i_4}-j_{i_3}-j_{i_5})}\delta K^{i_3i_2i_5i_4}_{k+q_y,\mathbf{q},k}$$

$$- |H_{j_{i_1}j_{i_3}}(q_{xy})||H_{j_{i_5}j_{i_4}}(q_{xy})|G^*_{m_{i_1}m_{i_3}}(q_z)G_{m_{i_5}m_{i_4}}(q_z)e^{-i(\pi/2)a_1}e^{-i\theta(j_{i_1}+j_{i_4}-j_{i_3}-j_{i_5})}\delta K^{i_2i_3i_4i_5*}_{k,\mathbf{q},k-q_y}], \tag{A6}$$

where the expression for a_2 is similar to a_1, with the exception that it contains index j_{i_2} instead of j_{i_1}.

Close inspection of Eqs. (A3) and (A6) shows that they represent independent identical subsystems of equations for each wave vector k, therefore the density matrix elements $f_{i_1i_2,k}$ and the quantities associated to the phonon-assisted matrices $\delta K^{i_1i_2i_4i_5}_{k,\mathbf{q},k-q_y}$ do not depend on the wave vector k under the influence of electron-LO phonon interaction alone. It is obvious from Eqs. (12) and (13) that the free electrons Hamiltonian and interaction with light do not introduce the dependence of phonon-assisted matrices on the wave vector k as well. Furthermore, since the thermal equilibrium of phonons is assumed, phonon populations do not depend on the wave vector $\mathbf{q}$, and neither does $\delta K^{i_1i_2i_4i_5}_{k,\mathbf{q},k-q_y}$ ($\delta K^{i_1i_2i_4i_5}_{k,\mathbf{q},k-q_y} \rightarrow \delta K_{i_1i_2i_4i_5}$). Consequently, we have

$$f_{i_1i_2,k} = \alpha_B n_{i_1i_2}, \quad \alpha_B = \frac{\pi\hbar}{eB}, \quad n_{i_1i_2} = \frac{\sum_{k'} f_{i_1i_2,k'}}{L_x L_y},$$

$$\frac{d}{dt}n_{i_1i_2}\bigg|_{\hat{H}_{ep}} = \frac{1}{i\hbar}\sum_{i_3,i_4,i_5,\mathbf{q}}|g_{\mathbf{q}}|^2[H_{j_{i_2}j_{i_3}}(q_{xy})||H_{j_{i_5}j_{i_4}}(q_{xy})|G_{m_{i_2}m_{i_3}}(q_z)G^*_{m_{i_5}m_{i_4}}(q_z)e^{i(\pi/2)a_2}e^{i\theta(j_{i_2}+j_{i_4}-j_{i_3}-j_{i_5})}\delta K_{i_1i_3i_4i_5}$$

$$+ |H_{j_{i_3}j_{i_2}}(q_{xy})||H_{j_{i_4}j_{i_5}}(q_{xy})|G^*_{m_{i_3}m_{i_2}}(q_z)G_{m_{i_4}m_{i_5}}(q_z)e^{i(\pi/2)a_2}e^{i\theta(j_{i_2}+j_{i_4}-j_{i_3}-j_{i_5})}\delta K^*_{i_3i_1i_5i_4}$$

$$- |H_{j_{i_3}j_{i_1}}(q_{xy})||H_{j_{i_4}j_{i_5}}(q_{xy})|G_{m_{i_3}m_{i_1}}(q_z)G^*_{m_{i_4}m_{i_5}}(q_z)e^{-i(\pi/2)a_1}e^{-i\theta(j_{i_1}+j_{i_4}-j_{i_3}-j_{i_5})}\delta K_{i_3i_2i_5i_4}$$

$$- |H_{j_{i_1}j_{i_3}}(q_{xy})||H_{j_{i_5}j_{i_4}}(q_{xy})|G^*_{m_{i_1}m_{i_3}}(q_z)G_{m_{i_5}m_{i_4}}(q_z)e^{-i(\pi/2)a_1}e^{-i\theta(j_{i_1}+j_{i_4}-j_{i_3}-j_{i_5})}\delta K^*_{i_2i_3i_4i_5}],$$

$$\frac{d}{dt}\delta K_{i_1i_2i_4i_5} = \frac{1}{i\hbar}(E_{i_2} + \hbar\omega_{LO} - E_{i_1})\delta K_{i_1i_2i_4i_5} - \gamma\delta K_{i_1i_2i_4i_5} + \frac{1}{i\hbar}[(n_0+1)n_{i_1i_5}(\delta_{i_4,i_2} - \alpha_B n_{i_4i_2}) - n_0 n_{i_4i_2}(\delta_{i_1,i_5} - \alpha_B n_{i_1i_5})], \tag{A7}$$

where the substitution $\alpha_B \delta K_{i_1i_2i_4i_5} \rightarrow \delta K_{i_1i_2i_4i_5}$ is introduced. It follows from Eq. (A5) that if the condition $j_{i_{1,2}} + j_{i_4} = j_{i_3} + j_{i_5}$ is fulfilled, then $a_{i_{1,2}} = 0$. Furthermore, using the identity

$$\int_{\theta=0}^{2\pi} d\theta e^{i(\pi/2)a_{1,2}} e^{i\theta(j_{1,2}+j_{i_4}-j_{i_3}-j_{i_5})} = e^{i(\pi/2)a_{1,2}} 2\pi \delta_{j_{1,2}+j_{i_4},j_{i_3}+j_{i_5}}, \tag{A8}$$

and summing over the phonon wave vector **q**, we finally get the expressions given by Eq. (16) in Sec. II A.

In order to perform the Markovian approximation, it is assumed that the dominant time dependence is given by the exponential in Eq. (A2) and therefore the value of electron populations can be taken out of the integral.[36,37] Also, the fast oscillations of polarizations must be taken into account,[36,37] resulting in

$$\delta s_{k,\mathbf{q},k-q_y}^{i_1 i_2} = -i\pi \sum_{i_4,i_5} g_{\mathbf{q}}^* H_{j_{i_5} j_{i_4}}^*(k,k-q_y,q_x) G_{m_{i_5} m_{i_4}}^*(q_z) \delta(E_{i_5} + \hbar\omega_{\text{LO}} - E_{i_4})$$

$$\times [(n_0+1)f_{i_1 i_5,k}(\delta_{i_4,i_2} - f_{i_4 i_2,k-q_y}) - n_0 f_{i_4 i_2,k-q_y}(\delta_{i_1,i_5} - f_{i_1 i_5,k})], \tag{A9}$$

where the δ function $\delta(E)$ is obtained in the limit $\lim_{\gamma\to 0} \hbar\gamma/\{\pi[(\hbar\gamma)^2+E^2]\}$.[36] Consequently, for the system with the discrete electronic spectra, a Lorentzian with FWHM of $2\hbar\gamma$ should be effectively used instead of the δ functions in the equations of motion in the Markovian and Boltzmann descriptions. Following the identical procedure as in the derivation of the quantum kinetic equations, we obtain the equations of motion in the Markov limit given by Eq. (18) in Sec. II A.

APPENDIX B

In this appendix we derive the expression for the lateral overlap integral $H_{j_f j_i}(k_f,k_i,q_x) = \int u_{j_f}^*[x-f(k_f)] e^{iq_x x} u_{j_i}[x-f(k_i)] dx$, with the harmonic oscillator wave function of the form

$$u_j(x) = \sqrt{\frac{\beta}{2^j j! \sqrt{\pi}}} H_j[\beta(x-x_0)] e^{-(\beta^2/2)(x-x_0)^2}, \tag{B1}$$

where $\beta = eB/\hbar$, $x_{0i}=k_i/\beta^2$, $x_{0f}=k_f/\beta^2$, and $k_i=k_f \mp q_y$ (the upper sign holds for phonon absorption and the lower one for emission). Inserting $t=x-x_{0f}$, $t_0=\frac{\mp q_y+iq_x}{2\beta^2}$, and $z=t-t_0$ into Eq. (B1), the lateral overlap integral may be transformed into

$$H_{j_f j_i}(k_f,k_f \mp q_y,q_x) = \frac{\beta}{\sqrt{\pi}} \frac{1}{\sqrt{2^{j_i+j_f} j_i! j_f!}} e^{iq_x x_{0f}} e^{-q_{xy}^2/4\beta^2} e^{\mp i(q_x q_y/2\beta^2)} \int dz H_{j_f}(\beta z + \beta t_0) H_{j_i}\left(\beta z + \beta t_0 \pm \frac{q_y}{\beta}\right) e^{-\beta^2 z^2}. \tag{B2}$$

In order to obtain the final expression for $H_{j_f j_i}(k_f,k_i,q_x)$, we use the following identity:

$$\int dx e^{-c^2 x^2} H_m(a+cx) H_n(b+cx) = \frac{2^n \sqrt{\pi} m! b^{n-m}}{c} L_m^{n-m}(-2ab), \quad n>m. \tag{B3}$$

In the case when $j_i < j_f$, by substituting $c=\beta^2$, $m=j_i$, $n=j_f$, $a=\beta t_0 \pm q_y/\beta$, and $b=\beta t_0$, Eq. (B2) takes the form

$$H_{j_f j_i}(k_f,k_f \mp q_y,q_x) = \frac{\beta}{\sqrt{\pi}} \frac{1}{\sqrt{2^{j_i+j_f} j_i! j_f!}} e^{iq_x x_{0f}} e^{-q_{xy}^2/4\beta^2} e^{\mp i(q_x q_y/2\beta^2)} \frac{2^{j_f} \sqrt{\pi} j_i! (\beta t_0)^{j_f-j_i}}{\beta^2} L_{j_i}^{j_f-j_i}\left[-2\left(\beta t_0 \pm \frac{q_y}{\beta}\right)\beta t_0\right]. \tag{B4}$$

Since the following identities

$$-2\left(\beta t_0 \pm \frac{q_y}{\beta}\right)\beta t_0 = \frac{q_{xy}^2}{2\beta^2}, \quad \beta t_0 = \frac{\mp q_y + iq_x}{2\beta} = \frac{q_{xy}}{2\beta} e^{i\arg(\mp q_y + iq_x)} \tag{B5}$$

hold, the final form of Eq. (B4) reads

$$H_{j_f j_i}(k_f,k_f \mp q_y,q_x) = |H_{j_f j_i}(q_{xy})| e^{i(q_x k_f/\beta^2)} e^{\mp i(q_x q_y/2\beta^2)} e^{i\arg(\mp q_y + iq_x)(j_f-j_i)}, \tag{B6}$$

where

$$|H_{j_f j_i}(q_{xy})| = \left(\frac{j_i!}{j_f!}\right)^{1/2} \left(\frac{q_{xy}^2}{2\beta^2}\right)^{(j_f-j_i)/2} L_{j_i}^{j_f-j_i}\left(\frac{q_{xy}^2}{2\beta^2}\right) e^{-q_{xy}^2/4\beta^2}. \tag{B7}$$

Similarly, if $j_i > j_f$, it can be shown that

$$H_{j_f j_i}(k_f,k_f \mp q_y,q_x) = |H_{j_f j_i}(q_{xy})| e^{i(q_x k_f/\beta^2)} e^{\mp i(q_x q_y/2\beta^2)} e^{i\arg(\pm q_y + iq_x)(j_i-j_f)}, \tag{B8}$$

with

$$|H_{j_f j_i}(q_{xy})| = \left(\frac{j_f!}{j_i!}\right)^{1/2} \left(\frac{q_{xy}^2}{2\beta^2}\right)^{(j_i-j_f)/2} L_{j_f}^{j_i-j_f}\left(\frac{q_{xy}^2}{2\beta^2}\right) e^{-q_{xy}^2/4\beta^2}. \tag{B9}$$

*eenis@leeds.ac.uk

[1] J. Faist, F. Capasso, D. L. Sivco, C. Sirtori, A. L. Hutchinson, and A. Y. Cho, Science **264**, 553 (1994).

[2] R. C. Iotti and F. Rossi, Appl. Phys. Lett. **78**, 2902 (2001).

[3] H. Callebaut, S. Kumar, B. S. Williams, and Q. Hu, Appl. Phys. Lett. **84**, 645 (2004).

[4] Z. Ikonić, R. W. Kelsall, and P. Harrison, Phys. Rev. B **69**, 235308 (2004).

[5] Z. Ikonić, P. Harrison, and R. W. Kelsall, J. Appl. Phys. **96**, 6803 (2004).

[6] D. Indjin, P. Harrison, R. W. Kelsall, and Z. Ikonić, J. Appl. Phys. **91**, 9019 (2002).

[7] R. C. Iotti and F. Rossi, Phys. Rev. Lett. **87**, 146603 (2001).

[8] R. C. Iotti and F. Rossi, Rep. Prog. Phys. **68**, 2553 (2005).

[9] R. C. Iotti, E. Ciancio, and F. Rossi, Phys. Rev. B **72**, 125347 (2005).

[10] A. Wacker, Phys. Rev. B **66**, 085326 (2002).

[11] S. C. Lee and A. Wacker, Phys. Rev. B **66**, 245314 (2002).

[12] F. Banit, S. C. Lee, A. Knorr, and A. Wacker, Appl. Phys. Lett. **86**, 041108 (2005).

[13] S. C. Lee, F. Banit, M. Woerner, and A. Wacker, Phys. Rev. B **73**, 245320 (2006).

[14] I. Waldmüler, W. W. Chow, E. W. Young, and M. C. Wanke, IEEE J. Quantum Electron. **42**, 292 (2006).

[15] H. Callebaut and Q. Hu, J. Appl. Phys. **98**, 104505 (2005).

[16] I. Waldmüler, J. Förstner, S. C. Lee, A. Knorr, M. Woerner, K. Reimann, R. A. Kaindl, T. Elsaesser, R. Hey, and K. H. Ploog, Phys. Rev. B **69**, 205307 (2004).

[17] I. Waldmüler, W. W. Chow, and A. Knorr, Phys. Rev. B **73**, 035433 (2006).

[18] S. Butscher, J. Förstner, I. Waldmüler, and A. Knorr, Phys. Status Solidi B **241**, R49 (2004).

[19] S. Butscher, J. Förstner, I. Waldmüller, and A. Knorr, Phys. Rev. B **72**, 045314 (2005).

[20] J. Li and C. Z. Ning, Phys. Rev. Lett. **91**, 097401 (2003).

[21] C. Becker, C. Sirtori, O. Drachenko, V. Rylkov, D. Smirnov, and J. Leontin, Appl. Phys. Lett. **81**, 2941 (2002).

[22] D. Smirnov, C. Becker, O. Drachenko, V. V. Rylkov, H. Page, J. Leotin, and C. Sirtori, Phys. Rev. B **66**, 121305(R) (2002).

[23] D. Smirnov, O. Drachenko, J. Leotin, H. Page, C. Becker, C. Sirtori, V. Apalkov, and T. Chakraborty, Phys. Rev. B **66**, 125317 (2002).

[24] C. Becker, A. Vasanelli, C. Sirtori, and G. Bastard, Phys. Rev. B **69**, 115328 (2004).

[25] K. Kempa, Y. Zhou, J. R. Engelbrecht, P. Bakshi, H. I. Ha, J. Moser, M. J. Naughton, J. Ulrich, G. Strasser, E. Gornik, and K. Unterrainer, Phys. Rev. Lett. **88**, 226803 (2002).

[26] K. Kempa, Y. Zhou, J. R. Engelbrecht, and P. Bakshi, Phys. Rev. B **68**, 085302 (2003).

[27] A. Leuliet, A. Vasanelli, A. Wade, G. Fedorov, D. Smirnov, G. Bastard, and C. Sirtori, Phys. Rev. B **73**, 085311 (2006).

[28] A. Vasanelli, A. Leuliet, C. Sirtori, A. Wade, G. Fedorov, D. Smirnov, G. Bastard, B. Vinter, M. Giovannini, and J. Faist, Appl. Phys. Lett. **89**, 172120 (2006).

[29] I. Savić, P. Harrison, V. Milanović, D. Indjin, Z. Ikonić, and V. D. Jovanović, Phys. Status Solidi B **242**, 1812 (2005).

[30] J. Radovanović, V. Milanović, Z. Ikonić, D. Indjin, and P. Harrison, J. Appl. Phys. **97**, 103109 (2005).

[31] I. Savić, Z. Ikonić, V. Milanović, N. Vukmirović, V. D. Jovanović, D. Indjin, and P. Harrison, Phys. Rev. B **73**, 075321 (2006).

[32] V. V. Bryskin and P. Kleinert, Phys. Rev. B **59**, 8152 (1999).

[33] K. El Sayed, J. A. Kenrow, and C. J. Stanton, Phys. Rev. B **57**, 12369 (1998).

[34] M. W. Wu and H. Haug, Phys. Rev. B **58**, 13060 (1998).

[35] L. D. Landau and E. M. Lifshitz, *Quantum Mechanics: Nonrelativistic Theory* (Pergamon, London, 1959).

[36] T. Kuhn, in *Theory of Transport Properties of Semiconductor Nanostructures*, edited by E. Schöll (Chapman and Hall, London, 1998).

[37] T. Kuhn and F. Rossi, Rev. Mod. Phys. **74**, 895 (2002).

[38] S. Živanović, V. Milanović, and Z. Ikonić, Phys. Rev. B **52**, 8305 (1995).

[39] H. Haug and S. W. Koch, *Quantum Theory of the Optical and Electronic Properties of Semiconductors* (World Scientific, Singapore, 2004).

[40] D. Calecki, J. F. Palmier, and A. Chomette, J. Phys. C **17**, 5017 (1984).

[41] H. C. Schneider, W. W. Chow, and S. W. Koch, Phys. Rev. B **70**, 235308 (2004).

[42] I. Savić, Z. Ikonić, N. Vukmirović, D. Indjin, P. Harrison, and V. Milanović, Appl. Phys. Lett. **89**, 011109 (2006).